PHILOSOPHICAL TRANSACTIONS A

royalsocietypublishing.org/journal/rsta

Research

Cite this article: Bashkirtseva I, Pankratov A, Slepukhina E, Tsvetkov I. 2020 Constructive role of noise and diffusion in an excitable slow–fast population system. *Phil. Trans. R. Soc. A* **378**: 20190253.
http://dx.doi.org/10.1098/rsta.2019.0253

Accepted: 17 November 2019

One contribution of 18 to a theme issue 'Patterns in soft and biological matters'.

Subject Areas:
mathematical modelling, biomathematics, differential equations

Keywords:
slow–fast system, random disturbances, diffusion, pattern formation

Author for correspondence:
E. Slepukhina
e-mail:
evdokiia.slepukhina@uni-hohenheim.de

Constructive role of noise and diffusion in an excitable slow–fast population system

I. Bashkirtseva[1], A. Pankratov[1], E. Slepukhina[2] and I. Tsvetkov[1]

[1]Ural Federal University, Ekaterinburg, Russian Federation
[2]University of Hohenheim, Stuttgart, Germany

ES, 0000-0003-3523-6147

We study the effects of noise and diffusion in an excitable slow–fast population system of the Leslie–Gower type. The phenomenon of noise-induced excitement is investigated in the zone of stable equilibria near the Andronov–Hopf bifurcation with the Canard explosion. The stochastic generation of mixed-mode oscillations is studied by numerical simulation and stochastic sensitivity analysis. Effects of the diffusion are considered for the spatially distributed variant of this slow–fast population model. The phenomenon of the diffusion-induced generation of spatial patterns-attractors in the Turing instability zone is demonstrated. The multistability and variety of transient processes of the pattern formation are discussed.

This article is part of the theme issue 'Patterns in soft and biological matters'.

1. Introduction

Many real processes combine subsystems with very different time scales. For such processes, mathematical models are slow–fast dynamical systems [1]. Even in deterministic cases, slow–fast systems exhibit complex phenomena such as mixed-mode oscillations, Canard explosion and excitability [2–7]. Details of the mathematical slow–fast analysis can be found in [8,9]. These phenomena are widely studied in neuronal dynamics [10–12]. Population systems can also exhibit slow–fast dynamics because of the differences in intrinsic biological parameters of interacting species [13–15].

In nonlinear systems, even weak noise can crucially change dynamical regimes [16–18]. Stochastic effects in slow–fast excitable systems attract a deal of attention

THE ROYAL SOCIETY PUBLISHING

from many researchers [1,19–22]. Well-known difficulties in describing stochastic dynamics using the Kolmogorov–Fokker–Planck equation in systems of dimension two and higher lead to the necessity to use asymptotic approximations [23,24]. One of the approaches for the construction of such approximations is based on the stochastic sensitivity function technique [25–27]. This technique was successfully used in the analysis of the stochastic excitability in neuronal dynamics [28,29], chemical kinetics [30] and population dynamics [31].

Another intriguing phenomenon in nonlinear systems is the diffusion-induced pattern formation [32,33]. Indeed, in distributed systems, in the presence of diffusion the steady homogeneous equilibrium can lose its stability with the birth of new non-homogeneous attractors-patterns. The phenomenon of the pattern formation in population systems was studied in [34–36].

In the present paper, we study the effects of random forcing and diffusion in a predator–prey model of the Leslie–Gower type. The deterministic behaviour of this slow–fast model was investigated in [37,38]. An attractive feature of this model is the Canard explosion of limit cycles.

In §2, for this deterministic system, we give a parametric description of the transition from the excitable equilibria to Canard-type cycles.

In §3, we study how random disturbances deform equilibrium dynamics. We show that random forcing generates mixed-mode oscillations with large-amplitude spikes similar to Canard cycles. The phenomenon of the noise-induced excitement is studied by means of changes of probabilistic distributions and interspike intervals. For the prediction of the onset of this phenomenon, we apply the stochastic sensitivity function technique and confidence ellipses.

In §4, we consider a spatially distributed variant of this slow–fast population model. We study how diffusion can transform the homogeneous equilibrium into the spatial wave-like patterns. The multistability and diversity of transient processes in this distributed model are discussed.

2. Deterministic model

Consider the population model [37,38]

$$\left.\begin{aligned} \dot{u} &= u(1-u) - \frac{auv}{u+b} \\ \text{and} \quad \dot{v} &= \delta v\left(1 - \frac{v}{u+c}\right), \end{aligned}\right\} \tag{2.1}$$

where u and v are dimensionless variables which stand for the density of the prey and the predator, respectively. The first equation contains the standard logistic term, and the interaction of populations of prey and predator is due to the Holling functional response of type II. The second equation describes the evolution of the prey. Here, the last modified Leslie–Gower term [39] measures the loss of predator population due to rarity of its favourite food. The additional constant c in the denominator normalizes the residual reduction of the population of the predator because of severe scarcity of the favourite food. The parameter a denotes the maximum value which *per capita* reduction rate of prey u can attain.

In system (2.1), constants a, b, c and δ are positive. Under the assumption that the predator reproduces much slower than the prey, the constant δ is supposed to be small. So, model (2.1) is the example of the slow–fast system.

The deterministic dynamics of system (2.1) is rather well studied. In [38], the behaviour of this system in the zone of Canard-type cycles was considered.

In the present paper, we show how random noise influences the system (2.1) dynamics. First, consider the main features of the deterministic dynamics of this system.

System (2.1) has non-trivial equilibrium $M(\bar{u}, \bar{v})$, where

$$\bar{u} = \frac{1}{2}\left(1 - a - b + \sqrt{(1-a-b)^2 - 4(ac-b)}\right), \quad \bar{v} = \bar{u} + c. \tag{2.2}$$

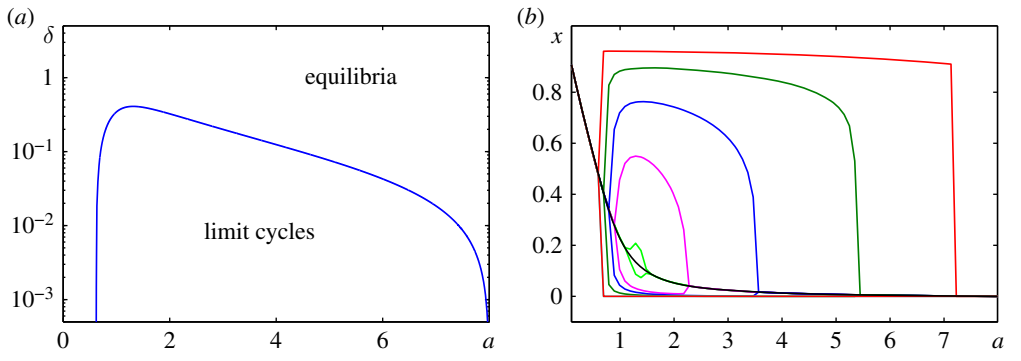

Figure 1. Deterministic system (2.1) with $b = 0.08$, $c = 0.01$: (*a*) bifurcation diagram, (*b*) attractors for $\delta = 0.5$ (black), $\delta = 0.4$ (light green), $\delta = 0.3$ (magenta), $\delta = 0.2$ (blue), $\delta = 0.1$ (dark green), $\delta = 0.01$ (red). (Online version in colour.)

This equilibrium belongs to the first quadrant if $ac - b < 0$. This equilibrium is stable if

$$1 - 2\bar{u} - \frac{ab(\bar{u} + c)}{(\bar{u} + b)^2} < \delta.$$

A parametric curve corresponding to the Andronov–Hopf bifurcation is defined as

$$\delta^* = 1 - 2\bar{u} - \frac{ab(\bar{u} + c)}{(\bar{u} + b)^2}.$$

Following [38], we fix $b = 0.08$, $c = 0.01$ and study system (2.1) dynamics with respect to a and δ. For these b and c, the equilibrium M belongs to the first quadrant if $0 < a < 8$.

In figure 1*a*, the Andronov–Hopf bifurcation line dividing zones of stable equilibria and stable limit cycles is plotted. Note that for $0 < a < 8$ and $\delta > 0.4086$, the system has only equilibria as attractors. For $0 < \delta < 0.4086$, on the interval $0 < a < 8$ two Andronov–Hopf bifurcations occur, so the system can exhibit both equilibria and stable limit cycles. As can be seen, the smaller the value of δ, the longer the $a-$parametric subinterval where self-oscillations are observed.

Extrema of u-coordinates of system (2.1) attractors are shown in figure 1*b* for six values of δ versus parameter a. For $\delta = 0.5$ (black), the system exhibits the stable equilibrium only. For $\delta = 0.4$ (light green), a small zone of self-oscillations is observed. Under decreasing δ, a size of the zone of limit cycles increases along with the increasing hardness of the Andronov–Hopf bifurcation. For example, for $\delta = 0.4$, the amplitude smoothly changes as the parameter varies. For $\delta = 0.01$, one can see a sharp change of the amplitude.

Details of such changes for u- and v-coordinates can be seen in figure 2. Here, $a_{AH} = 0.6282$ is the Andronov–Hopf bifurcation point. For $a > a_{AH}$, the amplitude of self-oscillations grows, but at the point $a_C = 0.6304$, a sharp jump can be observed. The value a_C localizes a so-called Canard explosion. Near a_C, the size of the limit cycle increases dramatically. This scenario is illustrated in figure 3 where the equilibrium and the limit cycles are shown for close values of the parameter a.

Undoubtedly, the phenomenon of the Canard explosion in system (2.1) with small δ is very attractive and important for the understanding of the unexpected nonlinear population dynamics. However, the system (2.1) with small δ exhibits interesting behaviour even in the zone of stable equilibria. Further, we fix $\delta = 0.01$ and study the system dynamics for varying a: $0 < a < a_{AH}$.

In figure 4*a*, a phase portrait of system (2.1) for $a = 0.625$ is plotted. Here, the stable equilibrium M has coordinates $\bar{u} = 0.45654$, $\bar{v} = 0.46654$. All phase trajectories tend to this equilibrium, but the transient process essentially depends on the deviation of the initial point from M. Indeed, for a small deviation (subthreshold zone), the trajectories tend to the equilibrium in a uniform manner. If the deviation exceeds some threshold value and initial state belongs to the superthreshold zone, the trajectory at first moves away from M, exhibits a large-amplitude 'excursion' and only after getting into the subthreshold zone starts to approach the equilibrium. Note that a form of this

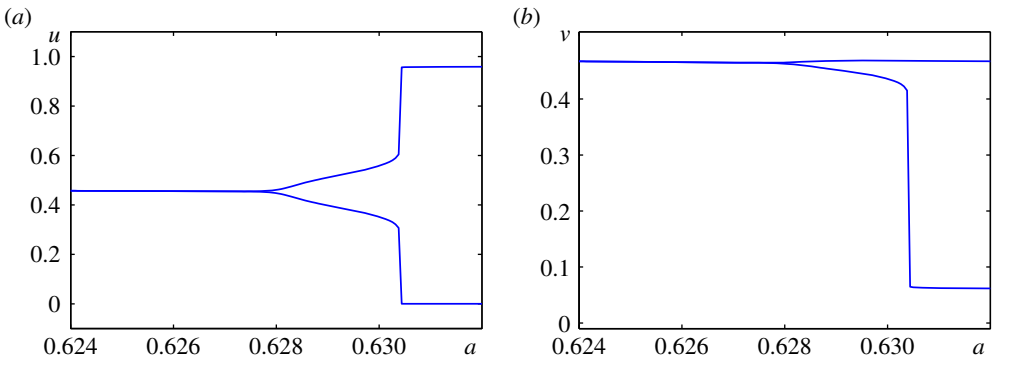

Figure 2. Extrema of attractors of system (2.1) for $\delta = 0.01$, $b = 0.08$, $c = 0.01$ near the Andronov–Hopf bifurcation point $a_{AH} = 0.6277$. (Online version in colour.)

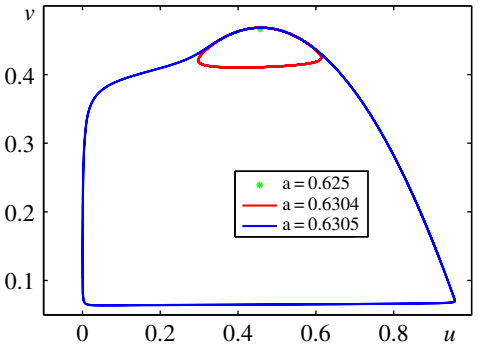

Figure 3. Canard explosion in system (2.1) with $\delta = 0.01$, $b = 0.08$, $c = 0.01$. (Online version in colour.)

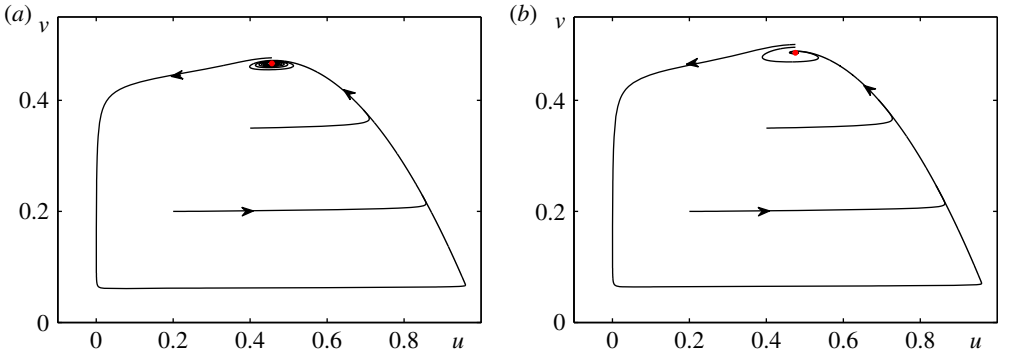

Figure 4. Phase portraits of system (2.1) with $\delta = 0.01$, $b = 0.08$, $c = 0.01$ and (*a*) $a = 0.625$, (*b*) $a = 0.6$. Stable equilibria are marked by red circles. (Online version in colour.)

loop is similar to the form of the Canard limit cycle (see blue curve in figure 3). A phase portrait of system (2.1) for $a = 0.6$ is plotted in figure 4*b*. This portrait is similar to the portrait shown in figure 4*a*, but there is an essential difference: the size of the subthreshold zone increases as the parameter a recedes from the bifurcation point a_{AH}.

These peculiarities of phase portraits of the deterministic model (2.1) are important for understanding the stochastic phenomena of the model taking into account the random disturbances.

3. Noise-induced excitability in stochastic model

For the analysis of the influence of random disturbances, we will use the following stochastic model:

$$\left.\begin{aligned} \dot{u} &= u(1-u) - \frac{(a+\varepsilon\xi)uv}{u+b} \\ \text{and} \qquad \dot{v} &= \delta v\left(1 - \frac{v}{u+c}\right). \end{aligned}\right\} \tag{3.1}$$

This model is obtained from the deterministic system (2.1) by replacing the deterministic parameter a by the following stochastic variant: $a \to a + \varepsilon\xi$. Here, $\xi(t)$ is a standard Gaussian white noise with parameters $\langle\xi(t)\rangle = 0$ and $\langle\xi(t)\xi(\tau)\rangle = \delta(t-\tau)$, and ε is the noise intensity.

Consider how random disturbances deform the deterministic dynamics in the zone of stable equilibria. For $a = 0.625$, results of stochastic forcing are illustrated in figure 5. For weak noise $\varepsilon = 0.002$, random trajectories starting from the deterministic equilibrium form small-amplitude stochastic oscillations (blue) around it. Here, stochastic trajectories lie in the subthreshold zone. For larger noise intensity $\varepsilon = 0.008$, random solutions fall into the superthreshold zone and start to exhibit mixed-mode stochastic oscillations of large and small amplitudes (green). In time series, one can see narrow spikes of almost equal amplitude. It should be noted that the population of the prey u demonstrates sharp deviations from the equilibrium up and down whereas the predator v deviates down only.

So, the system under random disturbances exhibits a phenomenon of the stochastic excitability in the parametric zone where the stable equilibrium is a single attractor.

Details of the stochastic excitement with transitions from small- to large-amplitude oscillations can be seen in figure 6 for two values of the parameter a. As one can see, the amplitude of the noise-induced spikes is almost independent of parameters a and ε. A difference is only in the noise intensity ε corresponding to the onset of the stochastic excitement: the smaller a, the greater ε.

For the parametric analysis of the phenomenon of noise-induced excitability, we will use a constructive approach based on the stochastic sensitivity functions technique and the confidence domains method [27,40]. For random states distributed around the stable equilibrium, a covariance matrix D can be approximated as $D \approx \varepsilon^2 W$, where W is a stochastic sensitivity matrix of this equilibrium.

The matrix W of the stochastic sensitivity for the equilibrium $M(\bar{u}, \bar{v})$ is a solution of the equation

$$FW + WF^{\top} = -S, \tag{3.2}$$

where F is the Jacobi matrix of system (2.1) at the equilibrium M and

$$S = \sigma \begin{bmatrix} 1 & 0 \\ 0 & 0 \end{bmatrix} \quad \text{and} \quad \sigma = \frac{\bar{u}^2\bar{v}^2}{(\bar{u}+b)^2}.$$

The stochastic sensitivity matrix W defines a corresponding confidence ellipse around the stable equilibrium M. The equation of this ellipse with the centre at the point $M(\bar{u}, \bar{v})$ can be written in the canonical form

$$\frac{z_1^2}{\lambda_1} + \frac{z_2^2}{\lambda_2} = -2\varepsilon^2 \ln(1-\mathcal{P}).$$

Here, λ_1, λ_2 are eigenvalues of the matrix W, z_1, z_2 are coordinates of the ellipse in the basis of normalized eigenvectors of W, and $\mathcal{P}$ is fiducial probability.

In figure 7, eigenvalues $\lambda_{1,2}$ ($\lambda_1 > \lambda_2$) of the stochastic sensitivity matrix W are plotted versus parameter a. As a approaches the bifurcation point a_{AH}, functions $\lambda_1(a)$, $\lambda_2(a)$ unlimitedly increase.

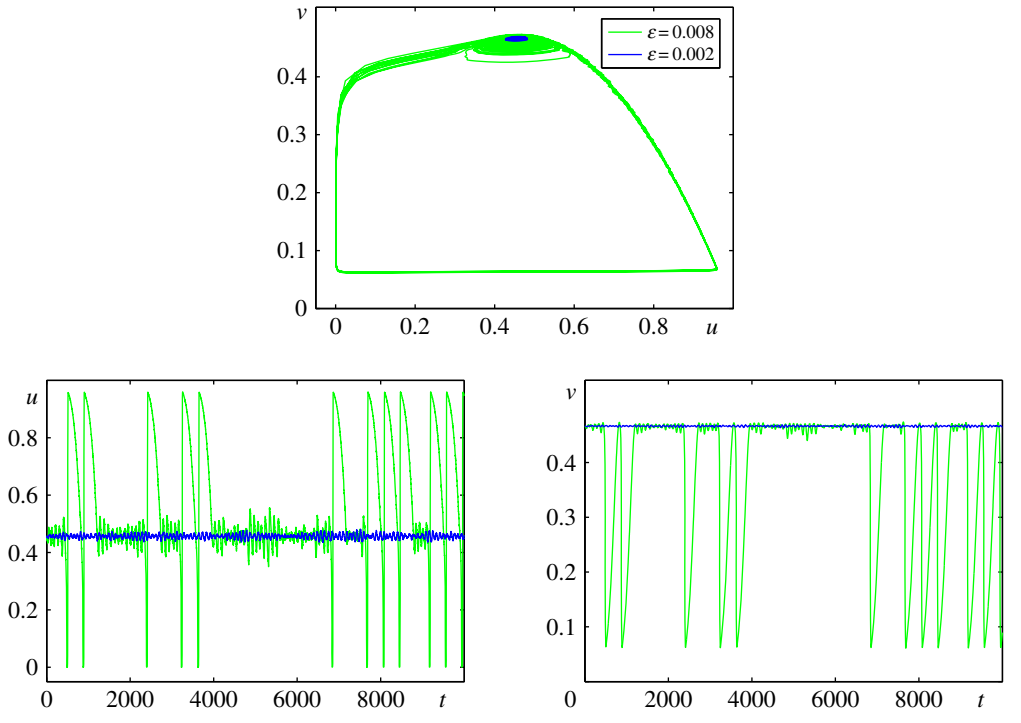

Figure 5. Stochastic excitability of the equilibrium in system (3.1) with $\delta = 0.01$, $b = 0.08$, $c = 0.01$ and $a = 0.625$. (Online version in colour.)

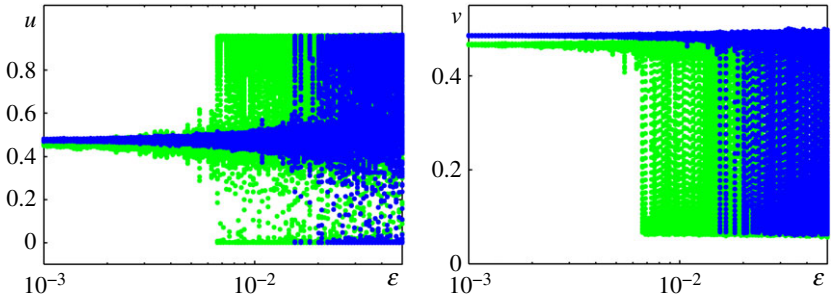

Figure 6. Random states of system (3.1) with $\delta = 0.01$, $b = 0.08$, $c = 0.01$ and $a = 0.6$ (blue), $a = 0.625$ (green). (Online version in colour.)

Values of $\lambda_1(a)$ are two orders greater than $\lambda_2(a)$, so the confidence ellipses have an essential eccentricity.

As is shown in figure 8, the confidence ellipse adequately describes a dispersion of random states of the stochastic system.

Confidence ellipses can be effectively used in the parametric analysis of the phenomenon of the noise-induced excitability. In figure 9*a*, for $a = 0.625$, confidence ellipses are plotted for $\varepsilon = 0.002$ (blue) and $\varepsilon = 0.008$ (green). A black phase curve of the deterministic system allows us to distinguish sub- and superthreshold zones. Here, small ellipse totally belongs to the subthreshold zone. It means that for $\varepsilon = 0.002$ stochastic trajectories reside inside the subthreshold zone and system (3.1) exhibits small-amplitude stochastic oscillations. As one can see, the large ellipse contains points of the superthreshold zone, so for $\varepsilon = 0.008$ stochastic trajectories fall down

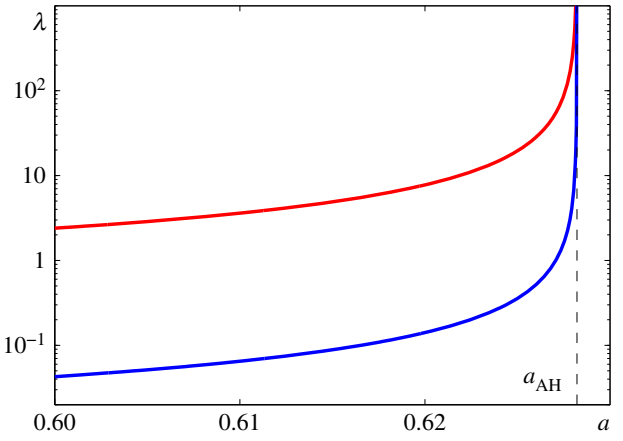

Figure 7. Stochastic sensitivity of the equilibria in system (3.1) with $\delta = 0.01$, $b = 0.08$, $c = 0.01$. (Online version in colour.)

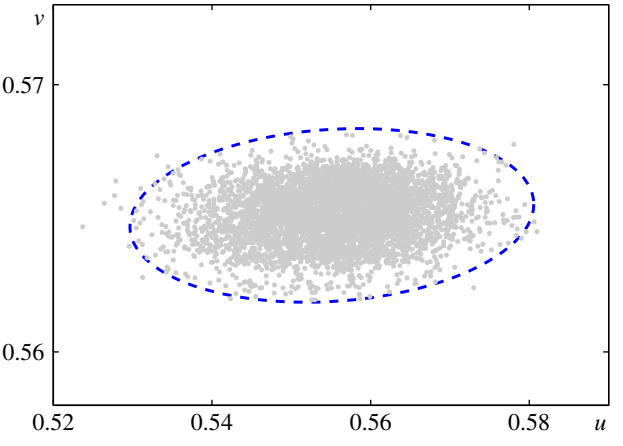

Figure 8. Random states (grey) and confidence ellipse (blue) for system (3.1) with $\delta = 0.01$, $b = 0.08$, $c = 0.01$, $a = 0.5$, and $\varepsilon = 0.01$. Here, fiducial probability is $\mathcal{P} = 0.99$. (Online version in colour.)

to the superthreshold zone and system (3.1) exhibits mixed-mode large-amplitude stochastic oscillations.

In figure 9*b*, a technique for the prediction of the noise-induced excitement with the help of the confidence ellipses is illustrated for $a = 0.6$. Here, the small ellipse (blue) corresponds to $\varepsilon = 0.01$ and the big one (green) is constructed for $\varepsilon = 0.04$. Comparing figure 9 and figure 6, one can see that the results of the theoretical prediction agree well with the direct numerical simulation. Indeed, noise-induced excitement (figure 6) occurs for the noise intensity estimated theoretically on the basis of confidence ellipses (figure 9).

Results of the quantitative extended parametric analysis of the stochastic excitability are presented in figures 10 and 11. In figure 10, mean values $m_u = \langle u \rangle$, $m_v = \langle v \rangle$ are plotted as functions of ε for three values of the parameter a. Here, one can see that the noise-induced excitement implies an increase of mean values m_u of the prey and a decrease of mean values m_v of the predator.

These plots show shifts of the mean values of the population densities whereas in figure 11 frequency characteristics of the noise-induced spiking can be seen. Here, we show how the mean values $\langle \tau \rangle$ of interspike intervals τ depend on the parameter a and the noise intensity ε. For weak

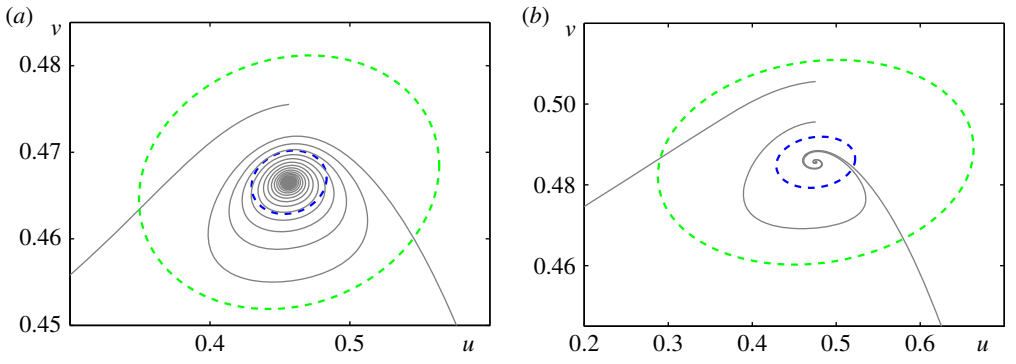

Figure 9. Confidence ellipses for system (3.1) with $\delta = 0.01$, $b = 0.08$, $c = 0.01$: (*a*) for $a = 0.625$ and $\varepsilon = 0.002$ (blue), $\varepsilon = 0.008$ (green), (*b*) for $a = 0.6$ and $\varepsilon = 0.01$ (blue), $\varepsilon = 0.04$ (green). Here, fiducial probability is $\mathcal{P} = 0.99$. (Online version in colour.)

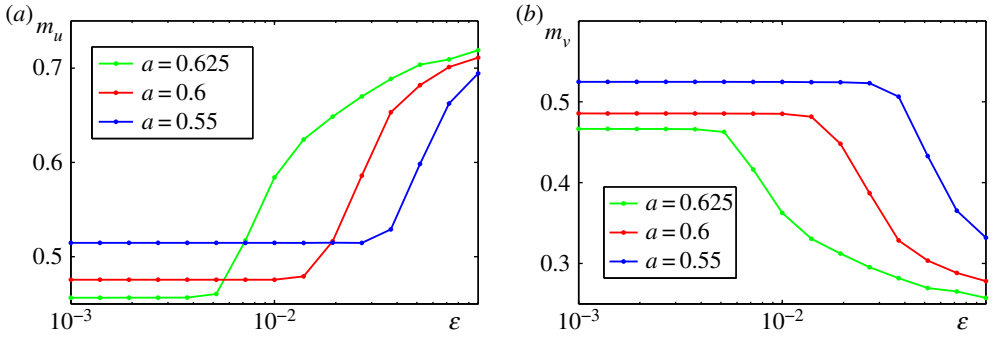

Figure 10. Mean values of u- and v-coordinates of solutions of system (3.1) with $\delta = 0.01, b = 0.08, c = 0.01$. (Online version in colour.)

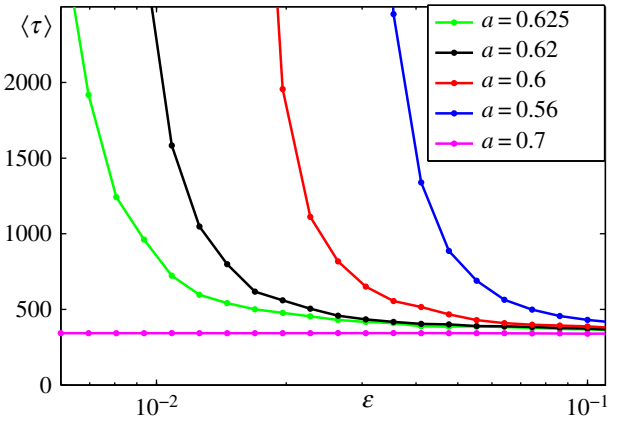

Figure 11. Mean values of the interspike intervals for system (3.1) with $\delta = 0.01, b = 0.08, c = 0.01$. (Online version in colour.)

noise, spikes are rare, so, mean values $\langle\tau\rangle$ are very large. As noise intensity increases, spikes become more frequent, so the mean value $\langle\tau\rangle$ monotonically decreases. An interesting feature of all curves in figure 11 is that all of them stabilize and almost coincide at $\varepsilon = 0.1$.

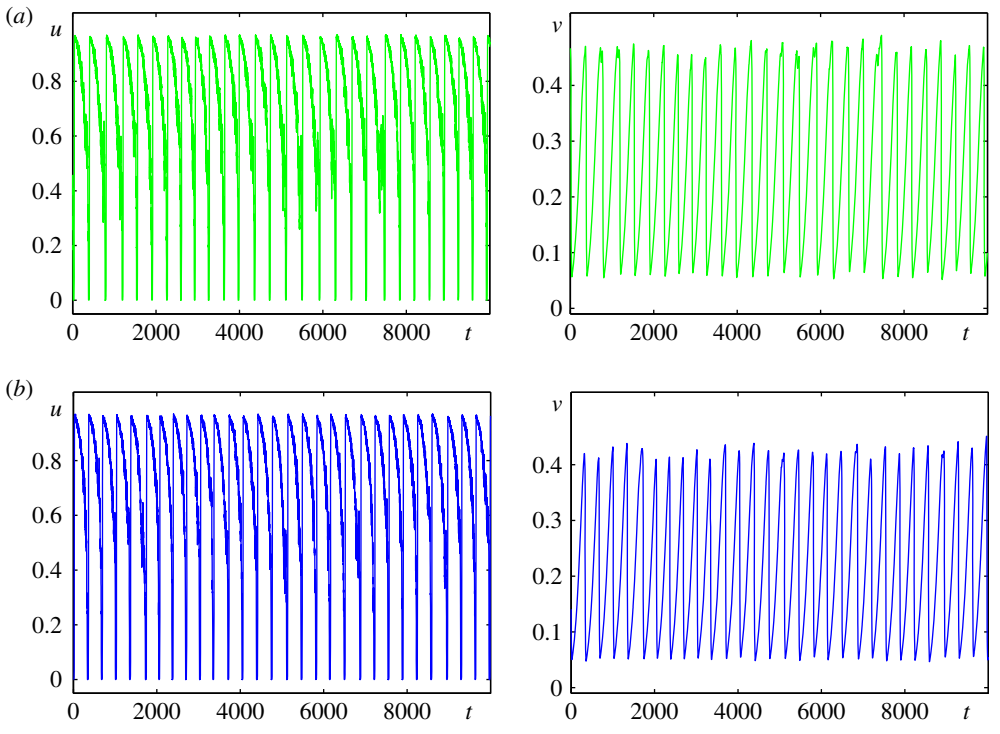

Figure 12. Time series of the stochastic system (3.1) with $\delta = 0.01$, $b = 0.08$, $c = 0.01$, $\varepsilon = 0.1$: (*a*) for $a = 0.625$, (*b*) for $a = 0.7$. (Online version in colour.)

In figure 11, we have also plotted $\langle \tau \rangle$ for $a = 0.7$ (magenta). For $a = 0.7$, the deterministic system demonstrates a stable limit cycle. The mean value $\langle \tau \rangle$ is almost constant and serves as an asymptote for all other curves from the zone of stable equilibria.

In figure 12 for $\varepsilon = 0.1$, we compare time series for $a = 0.625$ from the zone of stable equilibria and for $a = 0.7$ from the zone of stable cycles. As one can see in time series in figure 12*a*, a phase of the small-amplitude oscillations near the stable equilibrium almost disappears, and the stochastic system exhibits quasi-periodic large-amplitude stochastic oscillations. Time series in figure 12*b* are not much different from the curves in figure 12*a*.

Thus, in the presence of the noise, the population system can demonstrate the large-amplitude oscillatory regime despite the fact that its deterministic model predicts a stable equilibrium.

4. Spatial pattern formation in the model with diffusion

In this section, we consider a spatially distributed variant of the deterministic population model (2.1) with the diffusion. In the analysis of this distributed system, we focus on the case of one spatial variable

$$\left.\begin{aligned} \dot{u} &= u(1-u) - \frac{auv}{u+b} + D_u \frac{\partial^2 u}{\partial x^2} \\ \text{and} \quad \dot{v} &= \delta v \left(1 - \frac{v}{u+c}\right) + D_v \frac{\partial^2 v}{\partial x^2}. \end{aligned}\right\} \tag{4.1}$$

Let the following no-flux boundary conditions be assumed

$$\frac{\partial u}{\partial x}(t,0) = \frac{\partial u}{\partial x}(t,L) = \frac{\partial v}{\partial x}(t,0) = \frac{\partial v}{\partial x}(t,L) = 0.$$

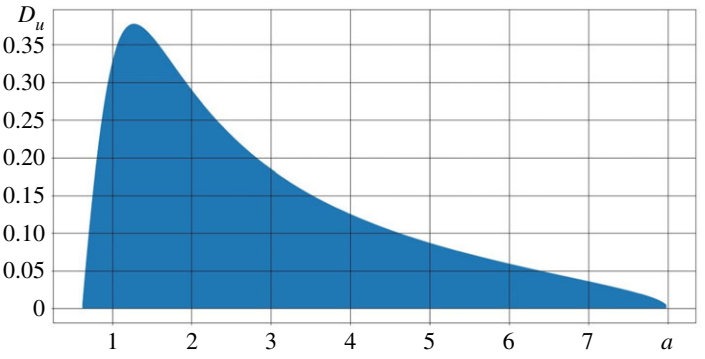

Figure 13. Bifurcation diagram of system (4.1) with $b = 0.08, c = 0.01, \delta = 0.5, D_v = 1$. (Online version in colour.)

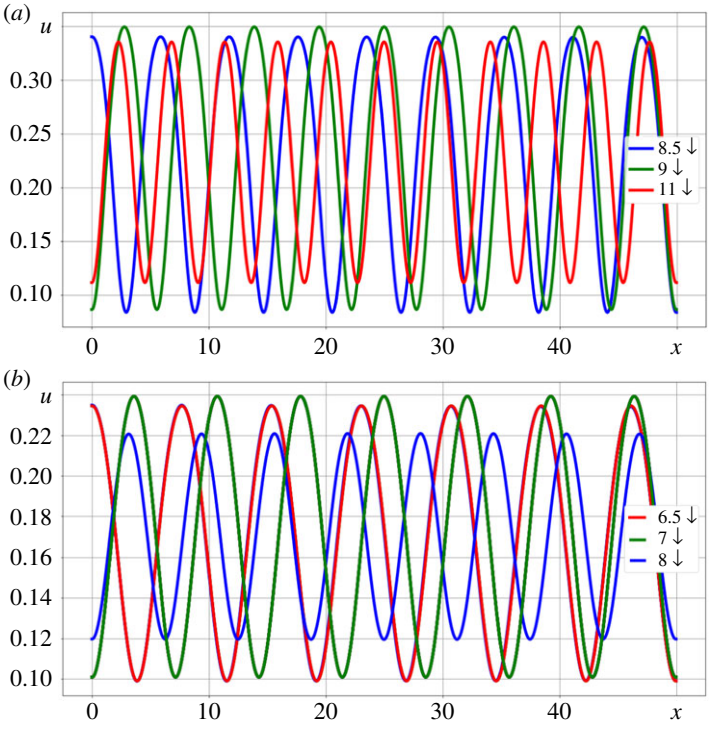

Figure 14. Spatial structures in system (4.1) with $a = 1, b = 0.08, c = 0.01, \delta = 0.5$: (*a*) for $D_u = 0.1$, (*b*) for $D_u = 0.2$. (Online version in colour.)

Here, functions $u(t, x)$, $v(t, x)$ are defined in $[0, +\infty) \times [0, L]$ and diffusion coefficients D_u, D_v are positive. These boundary conditions mean that both species do not cross the borders $x = 0$ and $x = L$.

Let $(\bar{u}, \bar{v})$ be a homogeneous steady solution of system (4.1) (see formulae (2.2)). It can be shown that the condition of the Turing instability [41] can be written in the following parametric form:

$$\sqrt{\frac{D_u}{D_v}} < \frac{\sqrt{\beta} - \sqrt{\beta - \alpha}}{\sqrt{\delta}},$$

where

$$\alpha = 1 - 2\bar{u} - \frac{ab\bar{v}}{(\bar{u} + b)^2} \quad \text{and} \quad \beta = \frac{a\bar{u}}{\bar{u} + b}.$$

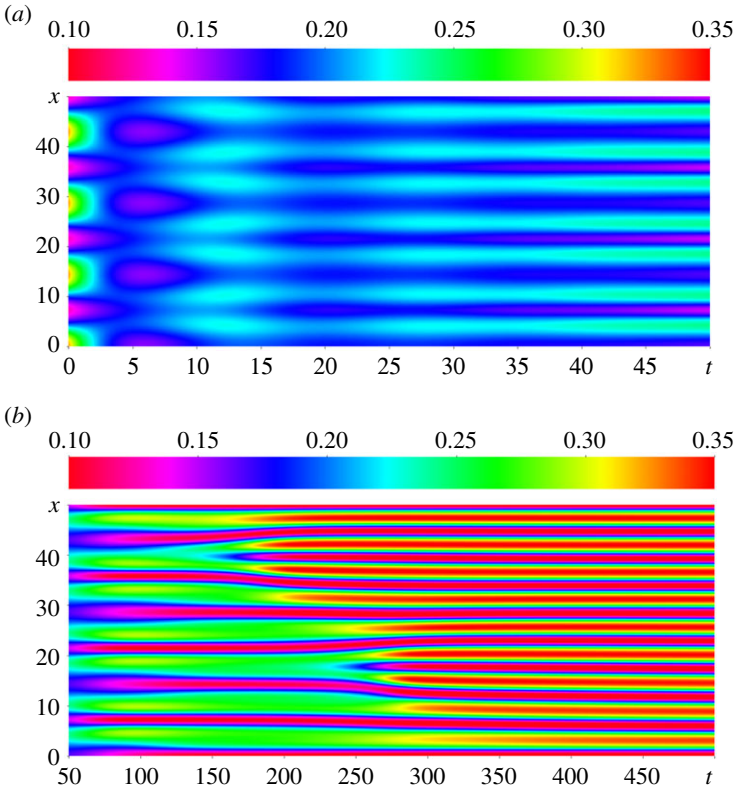

Figure 15. Transient process of u-coordinate in system (4.1) with $a = 1$, $b = 0.08$, $c = 0.01$, $\delta = 0.5$ from 3.5 $\downarrow$ pattern to 9 $\downarrow$ pattern for $D_u = 0.1$. (Online version in colour.)

Here, we fix

$$b = 0.08, \quad c = 0.01, \quad \delta = 0.5, \quad L = 50.$$

For these parameters (figure 1*b*), the non-distributed model (2.1) possesses the stable equilibrium $(\bar{u}, \bar{v})$ for any a. Let $D_v = 1$. In figure 13, (a, D_u)-parametric zone of the Turing instability is shown as shaded.

In the following, we fix $a = 1$, then the Turing bifurcation value is $D_u^* = 0.327$. So, the Turing instability zone is $0 < D_u < D_u^*$.

For numerical modelling values $u_{j,i} = u(t_j, x_i)$, $v_{j,i} = v(t_j, x_i)$ of solutions of system (4.1), the following scheme was used

$$u_{j+1,i} = u_{j,i} + \tau f_{j,i} + \tau D_u \frac{u_{j,i-1} - 2u_{j,i} + u_{j,i+1}}{h^2}$$

and

$$v_{j+1,i} = v_{j,i} + \tau g_{j,i} + \tau D_v \frac{v_{j,i-1} - 2v_{j,i} + v_{j,i+1}}{h^2}.$$

Here,

$$f_{j,i} = f(u_{j,i}, v_{j,i}), \quad g_{j,i} = g(u_{j,i}, v_{j,i})$$

and

$$f(u, v) = u(1 - u) - \frac{auv}{u + b}, \quad g(u, v) = \delta v \left(1 - \frac{v}{u + c}\right).$$

Numerical simulations of system (4.1) revealed that various spatially non-homogeneous stationary attractors-patterns are generated in the zone of Turing instability. The patterns in this

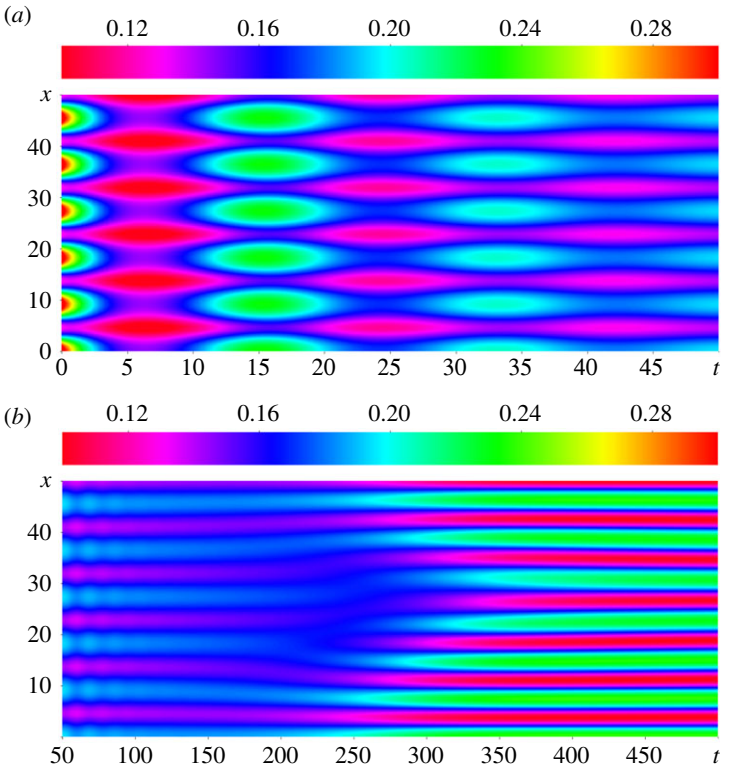

Figure 16. Transient process of u-coordinate in system (4.1) with $a = 1$, $b = 0.08$, $c = 0.01$, $\delta = 0.5$ from 5.5 ↓ pattern to 6.5 ↓ pattern for $D_u = 0.2$. (Online version in colour.)

zone are wave forms and can be simply characterized by the number of peaks and direction (↑ or ↓) near the right border $x = L$.

Some of the patterns are shown in figure 14 for $D_u = 0.1$ and $D_u = 0.2$. These patterns were obtained as steady solutions of system (4.1) starting from different initial states. So, the process of the self-organization in system (4.1) has an important feature, namely multistability. It should be noted that as the parameter D_u increases and approaches the Turing bifurcation value D_u^*, the amplitude of the spatial wave-patterns decreases.

It is also interesting to consider transient processes of the transformation of the initial state to the stationary non-homogeneous attractors. These transient processes are diverse.

Some examples demonstrating the complex process of pattern formation are presented in figures 15 and 16. In figure 15 for $D_u = 0.1$, it is shown how initial 3.5 ↓ structure transforms into 9 ↓ pattern. In the time interval $[0, 50]$, one can see the transition from the initial 3.5 ↓ wave to the intermediate 7 ↓ structure, so the doubling of the modality is observed. In the time interval $[50, 500]$, one can see more complicated non-homogeneous transformation of 7 ↓ wave into 9 ↓ pattern-attractor.

In figure 16 for $D_u = 0.2$, another type of transient process is shown. Here, the initial 5.5 ↓ wave undergoes homogeneous temporal oscillations with decreasing amplitude. For $t > 400$, the 6.5 ↓ pattern appears.

5. Conclusion

In this paper, we studied how noise and diffusion can cause qualitative changes in the behaviour of slow–fast population systems. As a conceptual slow–fast population model, a predator–prey

system of the Leslie–Gower type has been chosen. First, we studied the non-distributed model in equilibrium zone near the Andronov–Hopf bifurcation with the Canard explosion. It was shown how weak noise can generate large-amplitude oscillations similar to Canard cycles. This noise-induced excitement was analysed with the help of the confidence domains constructed via stochastic sensitivity functions. Second, we considered the phenomenon of diffusion-induced pattern formation in the distributed variant of this model. It was shown that the process of the spatial self-organization in this model demonstrates multistability and diversity of the transient processes.

Data accessibility. This article does not contain any additional data.
Authors' contributions. All authors contributed equally to this study.
Competing interests. We declare we have no competing interests.
Funding. The work was supported by Russian Science Foundation (grant no. 16-11-10098).

References

1. Berglund N, Gentz B. 2005 *Noise-induced phenomena in slow-fast dynamical systems: a sample-paths approach*. London, UK: Springer.
2. Peng B, Gaspar V, Showalter K. 1991 False bifurcations in chemical systems: canards. *Trans. R. Soc. Lond. A* **337**, 275–289. (doi:10.1098/rsta.1991.0123)
3. Brøns M, Krupa M, Wechselberger M. 2006 *Mixed mode oscillations due to the generalized canard phenomenon*. Providence, RI: American Mathematical Society, pp. 39–64.
4. Guckenheimer J, Haiduc R. 2005 Canards at folded nodes. *Mosc. Math. J.* **5**, 91–103. (doi:10.17323/1609-4514-2005-5-1-91-103)
5. Krupa M, Szmolyan P. 2001 Relaxation oscillation and canard explosion. *J. Differ. Equ.* **174**, 312–368. (doi:10.1006/jdeq.2000.3929)
6. Wechselberger M. 2005 Existence and bifurcation of Canards in R^3 in the case of a folded node. *SIAM J. Appl. Dyn. Syst.* **4**, 101–139. (doi:10.1137/030601995)
7. Desroches M, Guckenheimer J, Krauskopf B, Kuehn C, Osinga H, Wechselberger M. 2012 Mixed-mode oscillations with multiple time scales. *SIAM Rev.* **54**, 211–288. (doi:10.1137/100791233)
8. Fenichel N. 1979 Geometric singular perturbation theory for ordinary differential equations. *J. Differ. Equ.* **31**, 53–98. (doi:10.1016/0022-0396(79)90152-9)
9. Krupa M, Szmolyan P. 2001 Extending geometric singular perturbation theory to nonhyperbolic points-fold and canard points in two dimensions. *SIAM J. Math. Anal.* **33**, 286–314. (doi:10.1137/S0036141099360919)
10. Borgers C. 2017 *An introduction to modeling neuronal dynamics*. Berlin, Germany: Springer.
11. Izhikevich EM. 2007 *Dynamical systems in neuroscience: the geometry of excitability and bursting*. Cambridge, UK: MIT Press.
12. Drover J, Rubin J, Su J, Ermentrout B. 2004 Analysis of a canard mechanism by which excitatory synaptic coupling can synchronize neurons at low firing frequencies. *SIAM J. Appl. Math.* **65**, 69–92. (doi:10.1137/S0036139903431233)
13. Rinaldi S, Muratori S. 1992 Slow-fast limit cycles in predator-prey models. *Ecol. Modell.* **61**, 287–308. (doi:10.1016/0304-3800(92)90023-8)
14. Verhulst F. 2014 The hunt for canards in population dynamics: a predator-prey system. *Int. J. Non-Linear Mech.* **67**, 371–377. (doi:10.1016/j.ijnonlinmec.2014.10.017)
15. Dercole F, Ferriere R, Gragnani A, Rinaldi S. 2006 Coevolution of slow-fast populations: evolutionary sliding, evolutionary pseudo-equilibria and complex Red Queen dynamics. *Proc. R. Soc. B* **273**, 983–990. (doi:10.1098/rspb.2005.3398)
16. Horsthemke W, Lefever R. 1984 *Noise-induced transitions: theory and applications in physics, chemistry, and biology*. Berlin, Germany: Springer.
17. McDonnell MD, Stocks NG, Pearce CEM, Abbott D. 2008 *Stochastic resonance: from suprathreshold stochastic resonance to stochastic signal quantization*. Cambridge, UK: Cambridge University Press.
18. Gao JB, Hwang SK, Liu JM. 1999 When can noise induce chaos? *Phys. Rev. Lett.* **82**, 1132–1135. (doi:10.1103/PhysRevLett.82.1132)

19. Roberts A. 2008 Normal form transforms separate slow and fast modes in stochastic dynamical systems. *Physica A* **387**, 12–38. (doi:10.1016/j.physa.2007.08.023)
20. Lindner B, Garcia-Ojalvo J, Neiman A, Schimansky-Geier L. 2004 Effects of noise in excitable systems. *Phys. Rep.* **392**, 321. (doi:10.1016/j.physrep.2003.10.015)
21. Sieber M, Malchow H, Schimansky-Geier L. 2007 Constructive effects of environmental noise in an excitable prey-predator plankton system with infected prey. *Ecol. Complex.* **4**, 223–233. (doi:10.1016/j.ecocom.2007.06.005)
22. Bashkirtseva I, Ryashko L. 2018 Noise-induced shifts in the population model with a weak Allee effect. *Physica A* **491**, 28–36. (doi:10.1016/j.physa.2017.08.157)
23. Freidlin MI, Wentzell AD. 1984 *Random perturbations of dynamical systems*. New York, NY: Springer.
24. Milshtein GN, Ryashko LB. 1995 A first approximation of the quasipotential in problems of the stability of systems with random non-degenerate perturbations. *J. Appl. Math. Mech.* **59**, 47–56. (doi:10.1016/0021-8928(95)00006-B)
25. Bashkirtseva I, Ryashko L. 2002 Sensitivity analysis of stochastically forced Lorenz model cycles under period doubling bifurcations. *Dyn. Syst. Appl.* **11**, 293–310.
26. Bashkirtseva I, Ryashko L. 2014 Stochastic sensitivity of the closed invariant curves for discrete-time systems. *Physica A* **410**, 236–243. (doi:10.1016/j.physa.2014.05.037)
27. Bashkirtseva I. 2017 Stochastic sensitivity analysis: theory and numerical algorithms. *IOP Conf. Ser.: Mater. Sci. Eng.* **192**, 012024. (doi:10.1088/1757-899X/192/1/012024)
28. Bashkirtseva I, Neiman AB, Ryashko L. 2015 Stochastic sensitivity analysis of noise-induced suppression of firing and giant variability of spiking in a Hodgkin-Huxley neuron model. *Phys. Rev. E* **91**, 052920. (doi:10.1103/PhysRevE.91.052920)
29. Bashkirtseva I, Ryashko L, Slepukhina E. 2019 Noise-induced spiking-bursting transition in the neuron model with the blue sky catastrophe. *Phys. Rev. E* **99**, 062408. (doi:10.1103/PhysRevE.99.062408)
30. Bashkirtseva I, Ryashko L, Zaitseva S. 2019 Analysis of nonlinear stochastic oscillations in the biochemical Goldbeter model. *Commun. Nonlinear Sci. Numer. Simul.* **73**, 165–176. (doi:10.1016/j.cnsns.2019.02.008)
31. Bashkirtseva I, Ryashko L. 2018 Stochastic sensitivity analysis of noise-induced extinction in the Ricker model with delay and Allee effect. *Bull. Math. Biol.* **80**, 1596–1614. (doi:10.1007/s11538-018-0422-6)
32. Hoyle R. 2006 *Pattern formation: an introduction to methods*. Cambridge, UK: Cambridge University Press.
33. Cross M, Greenside H. 2009 *Pattern formation and dynamics in nonequilibrium systems*. Cambridge, UK: Cambridge University Press.
34. La Barbera A, Spagnolo B. 2002 Spatio-temporal patterns in population dynamics. *Physica A* **314**, 120–124. (doi:10.1016/S0378-4371(02)01173-1)
35. Baurmann M, Gross T, Feudel U. 2007 Instabilities in spatially extended predator-prey systems: spatio-temporal patterns in the neighborhood of Turing–Hopf bifurcations. *J. Theor. Biol.* **245**, 220–229. (doi:10.1016/j.jtbi.2006.09.036)
36. Malchow H, Petrovskii S, Venturino E. 2007 *Spatiotemporal patterns in ecology and epidemiology: theory, models, simulations*. Boca Raton, FL: Chapman & Hall/CRC Press.
37. Aziz-Alaoui M, Okiye MD. 2003 Boundedness and global stability for a predator-prey model with modified Leslie-Gower and Holling-type II schemes. *Appl. Math. Lett.* **16**, 1069–1075. (doi:10.1016/S0893-9659(03)90096-6)
38. Ambrosio B, Aziz-Alaoui MA, Yafia R. 2018 Canard phenomenon in a slow-fast modified Leslie-Gower model. *Math. Biosci.* **295**, 48–54. (doi:10.1016/j.mbs.2017.11.003)
39. Friedman A, Kao CY. 1977 *Mathematical ecology*. New York, NY: Wiley.
40. Bashkirtseva I, Ryashko L, Stikhin P. 2013 Noise-induced chaos and backward stochastic bifurcations in the Lorenz model. *Int. J. Bifurcation Chaos* **23**, 1350092. (doi:10.1142/S0218127413500922)
41. Turing AM. 1952 The chemical basis of morphogenesis. *Phil. Trans. R. Soc. Lond. B* **237**, 37–72. (doi:10.1098/rstb.1952.0012)